© 2016. Published by The Company of Biologists Ltd | Development (2016) 143, 2292-2304 doi:10.1242/dev.137844

RESEARCH REPORT

miR-219 regulates neural progenitors by dampening apical Par protein-dependent Hedgehog signaling

Laura I. Hudish[1], Domenico F. Galati[1], Andrew M. Ravanelli[1], Chad G. Pearson[1], Peng Huang[2] and Bruce Appel[1,*]

ABSTRACT

The transition of dividing neuroepithelial progenitors to differentiated neurons and glia is essential for the formation of a functional nervous system. Sonic hedgehog (Shh) is a mitogen for spinal cord progenitors, but how cells become insensitive to the proliferative effects of Shh is not well understood. Because Shh reception occurs at primary cilia, which are positioned within the apical membrane of neuroepithelial progenitors, we hypothesized that loss of apical characteristics reduces the Shh signaling response, causing cell cycle exit and differentiation. We tested this hypothesis using genetic and pharmacological manipulation, gene expression analysis and time-lapse imaging of zebrafish embryos. Blocking the function of miR-219, a microRNA that downregulates apical Par polarity proteins and promotes progenitor differentiation, elevated Shh signaling. Inhibition of Shh signaling reversed the effects of miR-219 depletion and forced expression of Shh phenocopied miR-219 deficiency. Time-lapse imaging revealed that knockdown of miR-219 function accelerates the growth of primary cilia, revealing a possible mechanistic link between miR-219-mediated regulation of apical Par proteins and Shh signaling. Thus, miR-219 appears to decrease progenitor cell sensitivity to Shh signaling, thereby driving these cells towards differentiation.

KEY WORDS: MicroRNA, Polarity, Hedgehog, Neural progenitors, Zebrafish

INTRODUCTION

Spatial and temporal information are integrated in developing nervous systems to produce a large array of distinct types of neurons and glia. In very broad terms, spatial cues specify formation of different kinds of neurons and glia at different positions whereas temporal information regulates the time at which particular dividing progenitor cells differentiate. One of the major spatial cues for developing vertebrate nervous systems is the secreted morphogen Sonic hedgehog (Shh). Shh binds to the cell surface transmembrane protein Patched (Ptch), relieving Ptch inhibition of the membrane spanning protein Smoothened (Smo). This initiates proteolytic processing of Gli transcription factors, which subsequently translocate to the nucleus to control expression of Hh pathway target genes (Aza-Blanc et al., 1997; Wang et al., 2000). Secretion of Shh by notochord, a mesodermal rod underlying the ventral neural tube and subsequently the floor plate – the ventral-most cells of the neural tube – creates a signaling gradient, to which neural progenitors arrayed on the ventral-to-dorsal axis respond by expressing position-specific transcription factors and producing distinct subsets of neurons and glia (Le Dréau and Martí, 2012; Jessell, 2000; Dessaud et al., 2008). For example, pMN progenitors, which are positioned close to the floor plate, express Olig2 and give rise to motor neurons and oligodendrocytes, whereas p2 progenitors slightly further from the Shh source, express Nkx6.1 and Irx3 and produce v2 interneurons and astrocytes.

Shh also functions as a mitogen, driving proliferation of neural progenitors (Ulloa and Briscoe, 2007). For instance, a recombinant N-terminal active fragment of Shh (Shh-N) elevated cell proliferation in cultured mouse retinas (Jensen and Wallace, 1997) and mouse cerebellar cell and slice cultures (Wechsler-Reya and Scott, 1999). Similarly, persistent expression of Shh in developing mouse spinal cord and cerebellum caused excess proliferation (Dahmane and Ruiz, 1999; Rowitch et al., 1999), and mice lacking functional Shh signaling inhibitors had larger neural tubes (Jeong and McMahon, 2005). Additionally, *Shh* mutant mice had significantly smaller neural tubes and general growth retardation (Litingtung and Chiang, 2000). Analysis of cell cycle regulation using cultured mouse cerebellar cells suggested that Shh can promote proliferation by upregulating signaling mediated by G1 cyclins (Kenney and Rowitch, 2000).

How do neural progenitors escape the mitogenic effect of Shh signaling to exit the cell cycle and differentiate? One possibility is that progenitors become less sensitive to Shh. During the early stages of neural development, progenitors have neuroepithelial characteristics, including apicobasal polarity. A prominent feature of this polarity is the assembly of protein complexes at the apical membrane. For example, the partioning-defective (Par) proteins Pard3, Pard6 and atypical protein kinase C iota (Prkci), form a complex that localizes to apical contact points between neuroepithelial cells (Afonso and Henrique, 2006; Chen and Zhang, 2013). In *Drosophila*, unequal distribution of apical Par polarity proteins maintains neuroblast fate during asymmetric divisions (Lee et al., 2006; Prehoda, 2009). Similarly, in mice, high levels of apical Par polarity proteins generally correlate with dividing neural progenitors and low levels with differentiation (Bultje et al., 2009; Costa et al., 2008; Kosodo et al., 2004). Notably, in vertebrate epithelial cells, Shh reception and signal processing occurs within primary cilia, which are cellular appendages positioned within the apical membrane (Ishikawa and Marshall, 2011). Recent evidence indicates that apical Par polarity proteins promote ciliogenesis (Fan et al., 2004; Krock and Perkins, 2014; Sfakianos et al., 2007). Together, these observations raise the possibility that apical Par proteins regulate the Shh signaling response in neural progenitors by regulating ciliogenesis.

We recently presented evidence that the microRNA miR-219 promotes differentiation of zebrafish neural progenitors at late stages of neural development by downregulating Pard3 and Prkci

[1]Departments of Pediatrics and Cell and Developmental Biology, University of Colorado School of Medicine, Aurora, CO 80045, USA. [2]Department of Biochemistry and Molecular Biology, University of Calgary, Calgary, Alberta, Canada, T2N 4N1.

*Author for correspondence (bruce.appel@ucdenver.edu)

A.M.R., 0000-0001-8138-3880; B.A., 0000-0003-4500-0672

Received 18 March 2016; Accepted 5 May 2016

Development (2016) 143, 2292-2304 doi:10.1242/dev.137844

(Hudish et al., 2013). However, the mechanisms by which apical Par proteins maintain neuroepithelial progenitors and how their downregulation promotes differentiation have not been determined. In this study, we tested the hypothesis that apical Par proteins maintain neuroepithelial progenitors by promoting their ability to respond to Hh signals. Our data show that miR-219-deficient embryos have elevated Hh signaling, which is dependent upon Par protein functions. Embryos lacking Par protein functions have decreased Hh signaling, which is not rescued by depleting miR-219, indicating that miR-219 regulation of Hh signaling occurs through Par protein regulation. We also show that miR-219 and Par proteins regulate the length and rate of growth of primary cilia. We propose that miR-219 helps to initiate the transition of progenitors from proliferation to differentiation by dampening apical Par protein-dependent Hh signal transduction, which might occur, at least in part, by regulating ciliogenesis.

RESULTS

miR-219 dampens Hh signaling

We previously showed that termination of neural progenitor divisions and subsequent neuronal and glial differentiation in zebrafish embryos is driven, in part, by negative regulation of Pard3 and Prkci by miR-219 (Hudish et al., 2013). Because Hh signaling is important for neural progenitor proliferation (Jensen and Wallace, 1997; Rowitch et al., 1999; Wechsler-Reya and Scott, 1999), we postulated that apical Par polarity proteins maintain neural progenitors by promoting responsiveness to Hh signals. To establish a baseline of Hh expression and response in zebrafish embryonic spinal cord, we used *in situ* RNA hybridization to detect expression of *sonic hedgehog a* (*shha*) and *patched2* (*ptch2*), which encodes a Hh receptor. Transcription of *ptch2* is increased with Hh signaling and *ptch2* RNA can therefore be a readout for Hh pathway activity (Concordet et al., 1996). Floor plate cells expressed *shha* at 1, 2 and 3 days post fertilization (dpf) (Fig. 1A-C). At 1 and 2 dpf, cells surrounding the primitive lumen, which extends across the dorsoventral axis of the neural tube, expressed *ptch2* (Fig. 1G,H). At 3 dpf, by which time the primitive lumen had transformed into a small, ventrally positioned central canal, only cells surrounding the central canal expressed *ptch2* (Fig. 1I). These observations indicate that during early neural development, spinal cord cells located distant from the floor plate are responsive to Hh signals, whereas later in development, Hh signaling is limited to cells in the ventral spinal cord. Notably, this transformation of the Hh response coincides with a loss of neuroepithelial characteristics, reduction in neural progenitor number and neuronal and glial differentiation in dorsal spinal cord (Hudish et al., 2013).

If miR-219 promotes neural progenitor differentiation by reducing apical Par polarity proteins and, consequently, Hh signaling, then miR-219-deficient embryos should have an altered Hh response. To test this prediction, we injected embryos with an antisense morpholino oligonucleotide (MO) designed to block the function of miR-219, which is expressed specifically in the neural tube (Zhao et al., 2010; Hudish et al., 2013). At 1, 2 and 3 dpf, spinal cord *shha* expression, revealed by *in situ* RNA hybridization, was similar in miR-219 MO-injected embryos (Fig. 1D-F) and control embryos (Fig. 1A-C). Similarly, *ptch2* expression appeared to be mostly unchanged by miR-219 MO injection at 1 and 2 dpf (Fig. 1J, K) compared with controls (Fig. 1G,H). However, at 3 dfp, *ptch2* RNA was evident more dorsally in miR-219 MO-injected embryos (Fig. 1L) compared with control embryos (Fig. 1I). To quantify the Hh signaling response, we used quantitative RT-PCR (qPCR) with a probe that measures the levels of *ptch2* RNA. This revealed that *ptch2* transcripts were more abundant in 3 dpf miR-219-deficient embryos than in control embryos (Fig. 1M). Additionally, we assessed the levels of RNA encoded by *gli1*, which is also a transcriptional target of Hh signaling activity (Rowitch et al., 1999). Embryos lacking miR-219 function had more *gli1* transcripts than control embryos (Fig. 1M). Finally, to measure the spatial distribution of *ptch2* expression within living embryos, we quantified the fluorescence localization profile of *Tg(ptch2:Kaede)* embryos, which express Kaede fluorescent protein under control of *ptch2* regulatory DNA (Huang et al., 2012). At 1 dpf, the shapes of the normalized fluorescence profiles were similar across the spinal cords of control and miR-219 MO-injected embryos (Fig. 1N,O,R,S,V). By contrast, the fluorescence profile was expanded in dorsal spinal cords of 3 dpf miR-219 MO-injected embryos relative to control embryos (Fig. 1P,Q,T,U,W). Together, these data indicate that miR-219-deficient embryos retain elevated Hh signaling in dorsal spinal cord into a late stage of embryonic development, consistent with the possibility that miR-219 reduces the Hh signaling response of neural progenitors.

miR-219 promotes loss of neural progenitor characteristics by reducing Hh signaling

We previously showed that reduction in miR-219 function resulted in maintenance of apical Par protein expression in the dorsal spinal cord and elevated numbers of proliferating neural progenitors (Hudish et al., 2013). Do these features of the miR-219 loss of function phenotype result from elevated Hh signaling? To test this possibility, we treated miR-219 MO-injected and control embryos with cyclopamine, a molecule that inhibits Hh pathway activation by binding to Smoothened (Chen et al., 2002). As expected, cyclopamine applied at 24 hpf nearly eliminated *ptch2* transcripts by 3 dpf (Fig. 3A). Treatment of wild-type embryos with cyclopamine beginning at 24 hpf did not change the localization of apical proteins ZO-1 (Fig. 2A,B,R) or Prkci (Fig. 2E,F,S), which both outlined the small, ventrally positioned central canal. Consistent with our previous data (Hudish et al., 2013), miR-219-deficient embryos had enlarged lumens that extended into the dorsal spinal cord and were outlined by apical ZO-1 (Fig. 2C) and Prkci localization (Fig. 2G). By contrast, lumen size and apical protein localization in miR-219 MO-injected embryos treated with cyclopamine were more similar to that of wild-type control embryos (Fig. 2D,H). To quantify these changes, we categorized the dorsal extent of ZO-1 and Prkci lumenal localization as severe, mild and normal. Similar to our previous findings (Hudish et al., 2013), ZO-1 and Prkci lumenal localization extended into the dorsal spinal cords of miR-219 MO-injected embryos, which we categorized as severe phenotypes (Fig. 2R,S). By contrast, miR-219 MO-injected embryos treated with Cyclopamine had milder ZO-1 and Prkci localization phenotypes (Fig. 2R,S). These data raise the possibility that high levels of Hh signaling maintain neuroepithelial characteristics, including apical membrane protein localization, in the dorsal spinal cord.

To test whether or not the excess number of neural progenitors of miR-219-deficient embryos also results from elevated Hh signaling, we performed immunohistochemistry to detect expression of Sox2, a marker of neural progenitors (Ellis et al., 2004). In 3 dpf wild-type embryos, $Sox2^+$ cells surrounded the central canal and occupied intermediate positions of the spinal cord, just dorsal to the central canal (Fig. 2I). Wild-type embryos treated with Cyclopamine from 24 hpf had similar numbers of $Sox2^+$ cells (Fig. 2J,T). Similar to our previous report (Hudish et al., 2013), miR-219 MO-injected embryos had more $Sox2^+$ cells and these were distributed across the dorsoventral axis of the spinal cord (Fig. 2K,T). Cyclopamine-treated miR-219 MO-

Development (2016) 143, 2292-2304 doi:10.1242/dev.137844

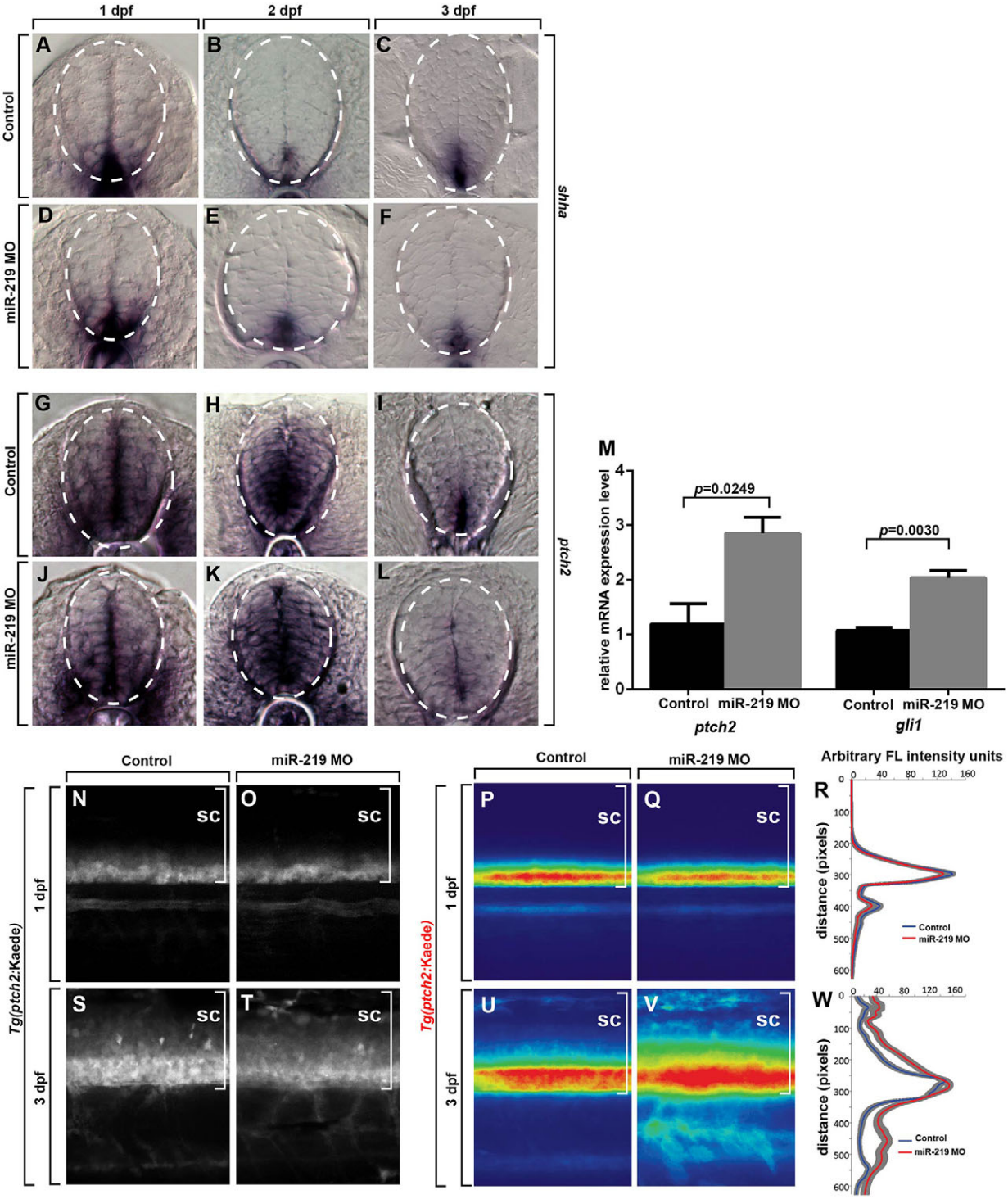

Fig. 1. Reduction of miR-219 causes persistent Hh signaling. (A-L) Representative transverse sections through trunk spinal cord with dorsal up. Dashed circles outline spinal cords. *In situ* RNA hybridization to detect *shha* in wild-type embryos (A-C) and miR-219 MO-injected embryos (D-F) at 1, 2 and 3 dpf (G-I). *In situ* RNA hybridization to detect *ptch2* transcripts in wild-type embryos reveals expression throughout the entire dorsoventral axis of the spinal cord at 1 and 2 dpf. By 3 dpf, expression is confined to an area bordering the ventrally located central canal. (J-L) miR-219 MO-injected embryos processed to detect *ptch2* RNA. *ptch2* expression appears to persist in dorsal spinal cord of the miR-219-deficient embryo (L). (M) Graph showing that 3 dpf miR-219 MO-injected larvae express *ptch2* and *gli1* RNA at higher levels than stage-matched controls. Data represent the mean±s.e.m. (n=3 biological replicate experiments, consisting of 15-20 larvae, each). Significance calculated using an unpaired t-test. (N-Q) Representative maximum projection images of confocal images stacks of *ptch2*:Kaede expression in control and miR-219 MO-injected embryos at 1 dpf (N,O) and 3 dpf (P,Q). (R-U) Heat maps showing the average normalized fluorescence profile of spinal cord (sc, brackets) *ptch2*:Kaede at 1 dpf (n=22 control embryos and 20 miR-219 MO-injected embryos) (R,S) and 3 dpf (n=22 control and 18 miR-219 MO-injected) (T,U), straightened and aligned along the dorsoventral axis, with dorsal to the top. All heat maps display in the range of 0-150 arbitrary fluorescence intensity units (blue to red). (V,W) Average normalized fluorescence profile of *ptch2*:Kaede fluorescence generated by creating line scans along the dorsoventral axis. The solid colored lines (red and blue) represent the average normalized fluorescence profile at each pixel along the dorsoventral axis of 1 dpf (R) and 3 dpf (W) spinal cords, whereas the grey lines represent the s.e.m. at each pixel.

Development (2016) 143, 2292-2304 doi:10.1242/dev.137844

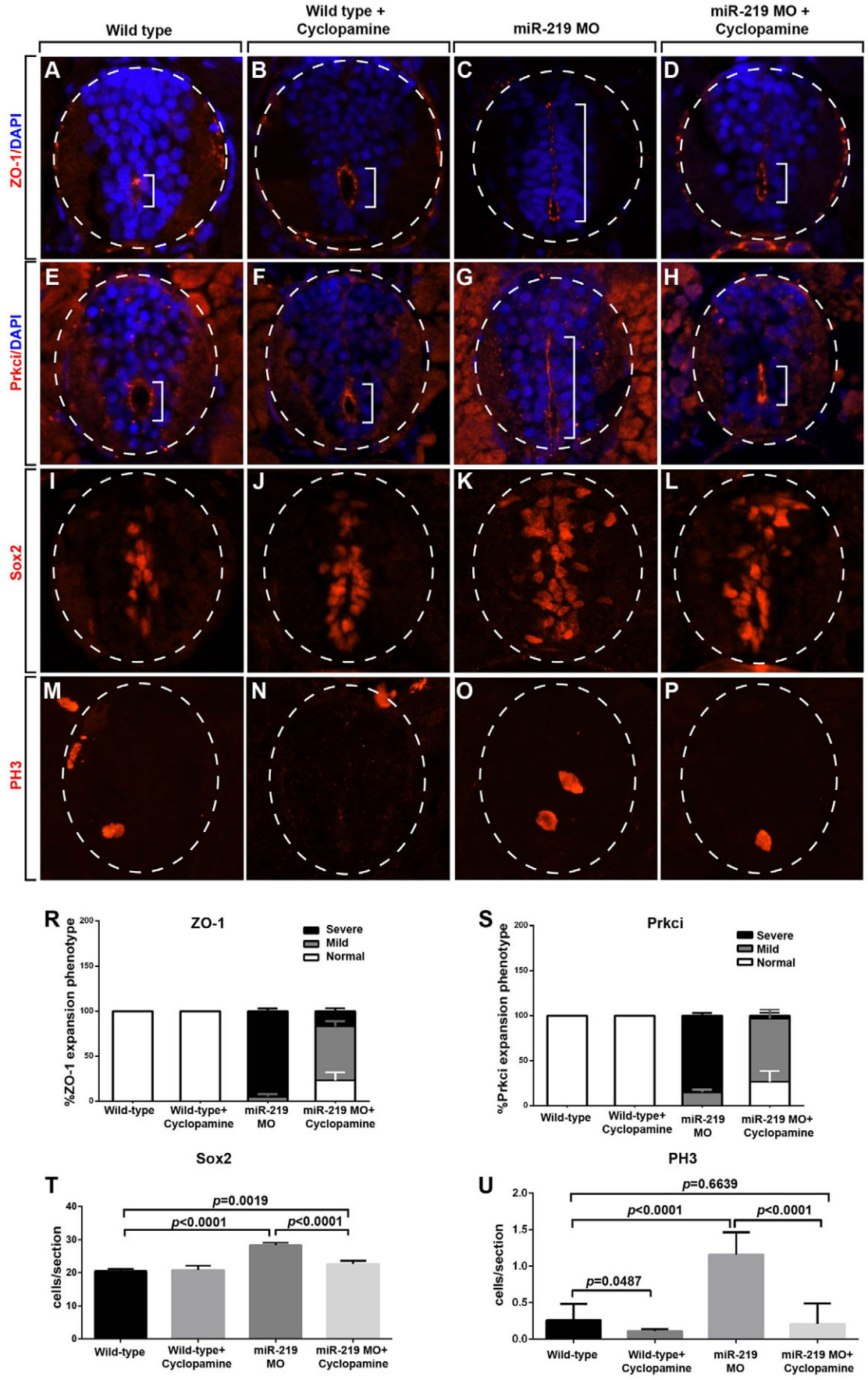

Fig. 2. See next page for legend.

Development (2016) 143, 2292-2304 doi:10.1242/dev.137844

Fig. 2. miR-219-mediated neural progenitor maintenance requires Hh signaling. (A-P) Representative transverse sections through trunk spinal cords of 3 dpf embryos with dorsal up. Dashed circles outline spinal cords and brackets indicate central canals/primitive lumens highlighted by ZO-1 and Prkci localization. ZO-1 (A-D) and Prkci (E-H) localization at apical membranes detected by immunohistochemistry. In wild-type (A,E) and cyclopamine-treated wild-type (B,F) embryos, ZO-1 and Prkci are localized to apical membranes surrounding a small, ventrally positioned central canal. miR-219 MO-injected embryos have primitive lumens, decorated by ZO-1 and Prkci, that extend across the dorsoventral length of the spinal cord (C,G). Cyclopamine treatment suppresses the lumenal and apical protein localization phenotype of miR-219 MO-injected embryos (D,H). (I-L) Spinal cord progenitors revealed by Sox2 immunohistochemistry. Cyclopamine treatment suppresses the excess progenitor phenotype of miR-219 MO-injected embryos. (M-P) Dividing spinal cord cells revealed by PH3 immunohistochemistry. Cyclopamine treatment suppresses the excess dividing cell phenotype of miR-219 MO-injected embryos. (R) Graph showing quantification of the ZO-1 phenotype. Embryos classified as normal had ZO-1 expression around the ventrally located central canal. Embryos were classified as severe when ZO-1 localization spanned the entire dorsoventral axis and mild when it spanned an intermediate length. Data represent the mean±s.e.m. (n=15 larvae for each group). P values were calculated by comparing the numbers of larvae with severe and mild phenotypes in miR-219 MO alone and the miR-219 MO+cyclopamine experiments. P<0.0001 for the severe group and P=0.0062 for the mild group, unpaired t-test. (S) Graph showing quantification of the Prkci phenotype. Embryos were scored as in R. Data represent the mean±s.e.m. (n=15 larvae for each group). P<0.001 for the severe group and P=0.0033 for the mild group, unpaired t-test. (T) Graph showing the number of $Sox2^+$ progenitors. Data represent the mean±s.e.m. (n=15 embryos per group). Significance calculated using an unpaired t-test. (U) Graph showing the number of $PH3^+$ cells in wild-type control, wild-type+cyclopamine, miR-219 MO and miR-219 MO+cyclopamine larvae. Data represent the mean±s.e.m. (n=15 sections obtained from 5 larvae per group, with three replicates). Significance calculated using an unpaired t-test.

injected embryos had fewer $Sox2^+$ cells compared with untreated miR-219 MO-injected embryos, but slightly more than control and cyclopamine-treated wild-type embryos (Fig. 2L,T). Furthermore, immunohistochemistry to detect phosphohistone H3 (PH3), which reveals cells in mitosis, showed that whereas miR-219 MO-injected embryos had significantly more $PH3^+$ cells than control embryos (Fig. 2M-O), cyclopamine-treated miR-219 MO-injected embryos had approximately the same number of $PH3^+$ cells as control embryos (Fig. 2P,U). Thus, Hh inhibition suppressed the excess neural progenitor phenotype of miR-219-deficient embryos, consistent with the possibility that miR-219 promotes neural progenitor cell cycle exit and differentiation, at least in part, by dampening Hh signaling.

To further investigate the relationship between miR-219 function and Hh signaling, we tested the prediction that artificially elevating Shh expression would phenocopy the loss of miR-219 function. To do so, we used the transgenic line *Tg(hsp701:Shha:EGFP)* (Shen et al., 2013), which expresses Shh fused to EGFP under the control of heat-responsive DNA elements, to temporally regulate Hh signaling levels (Shh HS). We allowed the embryos to develop normally until 1 dpf after which they were placed twice daily at a higher temperature until 3 dpf to induce transgene expression. As expected, Shh overexpression resulted in elevated levels of *ptch2* mRNA (Fig. 3A) and expansion of the *ptch2:*Kaede reporter along the dorsoventral spinal cord axis (Fig. 3B-D). At 3 dpf, $Sox2^+$ cells lined the ventral central canal of control embryos (Fig. 3E). By contrast, Shh-overexpressing embryos had an excess of $Sox2^+$ cells, which lined the entire dorsoventral axis of the medial spinal cord (Fig. 3F). Quantification of the $Sox2^+$ cells revealed a twofold increase in Shh-overexpressing embryos when compared with the control (Fig. 3G). Additionally, spinal cord cells of embryos induced to express Shh-EGFP incorporated more EdU, a thymidine analog used to detect cells in S phase of the cell cycle, than control embryos did (Fig. 3H-J). The spinal cord lumens of embryos induced to express Shh-EGFP were enlarged and outlined by apical ZO-1 (Fig. 3K,L) and Prkci localization (Fig. 3M,N), indicating that more cells maintained apical membrane. Thus, similar to loss of miR-219 function, prolonged and elevated Shh expression maintained neuroepithelial characteristics, consistent with the possibility that miR-219 negatively regulates Hh signaling.

Apical Par proteins mediate the effects of miR-219 on Hh signaling

Our data are consistent with an interpretation that miR-219 drives cell cycle exit and loss of neural progenitor characteristics by dampening Hh signaling. Previously, we presented evidence the miR-219 negatively regulates the apical Par polarity proteins Pard3 and Prkci (Hudish et al., 2013). Together, these observations raise the possibility that miR-219 suppresses Hh signaling in the neural tube by suppressing Pard3 and Prkci. To investigate this possibility, we blocked access to the miR-219 target site on both *pard3* and *prkci* 3′UTRs. To do this, we used target protector MOs (TP MOs), which bind to the miR-219 target sites on either *pard3* or *prkci* mRNAs (Hudish et al., 2013), rendering miR-219 unable to bind to *pard3* or *prkci* mRNAs. At 3 dpf, *pard3* TP MO-injected embryos expressed *ptch2* RNA in dorsal spinal cord, in contrast to control embryos where only cells lining the central canal expressed *ptch2* RNA (Fig. 4A,B). Although *prkci* TP MO had little apparent effect on the distribution of *ptch2* RNA assessed by RNA *in situ* hybridization (Fig. 4C), qPCR revealed that embryos injected with *pard3* TP MO and *prkci* TP MO had significantly elevated levels of *ptch2* and *gli1* transcripts (Fig. 4D). Therefore, blocking interaction of miR-219 with its *pard3* or *prkci* target sites elevated *ptch2* and *gli1* transcript levels, supporting the hypothesis that maintenance of apical Par proteins promotes Hh signaling levels.

Our data indicate that elevated expression of Pard3 and Prkci in miR-219-deficient embryos elevates Hh signaling in the spinal cord. To investigate whether or not apical Par protein functions are necessary for Hh signaling, we first compared *ptch2* RNA expression in wild-type and *prkci* mutant (Horne-Badovinac et al., 2001) embryos. Cells along the entire dorsoventral axis expressed *ptch2* RNA in wild-type embryos at 2 dpf (Fig. 4E), whereas only a few cells located in the ventral spinal cords of 2 dpf *prkci* mutant embryos expressed *ptch2* RNA (Fig. 4F). By 3 dpf, only cells in the ventral spinal cord of wild-type embryos expressed *ptch2* RNA (Fig. 4G) and 3 dpf *prkci* mutant embryos expressed little or no *ptch2* RNA (Fig. 4H). Thus, Prkci function is necessary for Hh signaling in the spinal cord, consistent with the possibility that modulation of apical Par protein levels by miR-219 modulates the Hh signaling level. To determine whether or not the elevated Hh signaling of miR-219-deficient embryos results from elevated apical Par protein levels, we injected miR-219 MO into *prkci* mutant embryos. In contrast to miR-219 MO-injected wild-type embryos, which expressed *ptch2* at elevated levels (Fig. 1L), miR-219 MO-injected *prkci* mutant embryos expressed *ptch2* similar to non-injected *prkci* mutant embryos (Fig. 4I). To further test this hypothesis we assessed transcript levels of *ptch2* and *gli1* by qPCR. Reduction of miR-219 in *prkci* mutant embryos had little to no impact on *ptch2* or *gli1* mRNA levels (Fig. 4J), supporting the hypothesis that miR-219 modulates Hh signaling levels through its regulation of apical Par proteins. Together with the data presented above, these results provide evidence that miR-219 dampens Hh signaling in the zebrafish spinal cord by reducing apical Par protein levels.

Development (2016) 143, 2292-2304 doi:10.1242/dev.137844

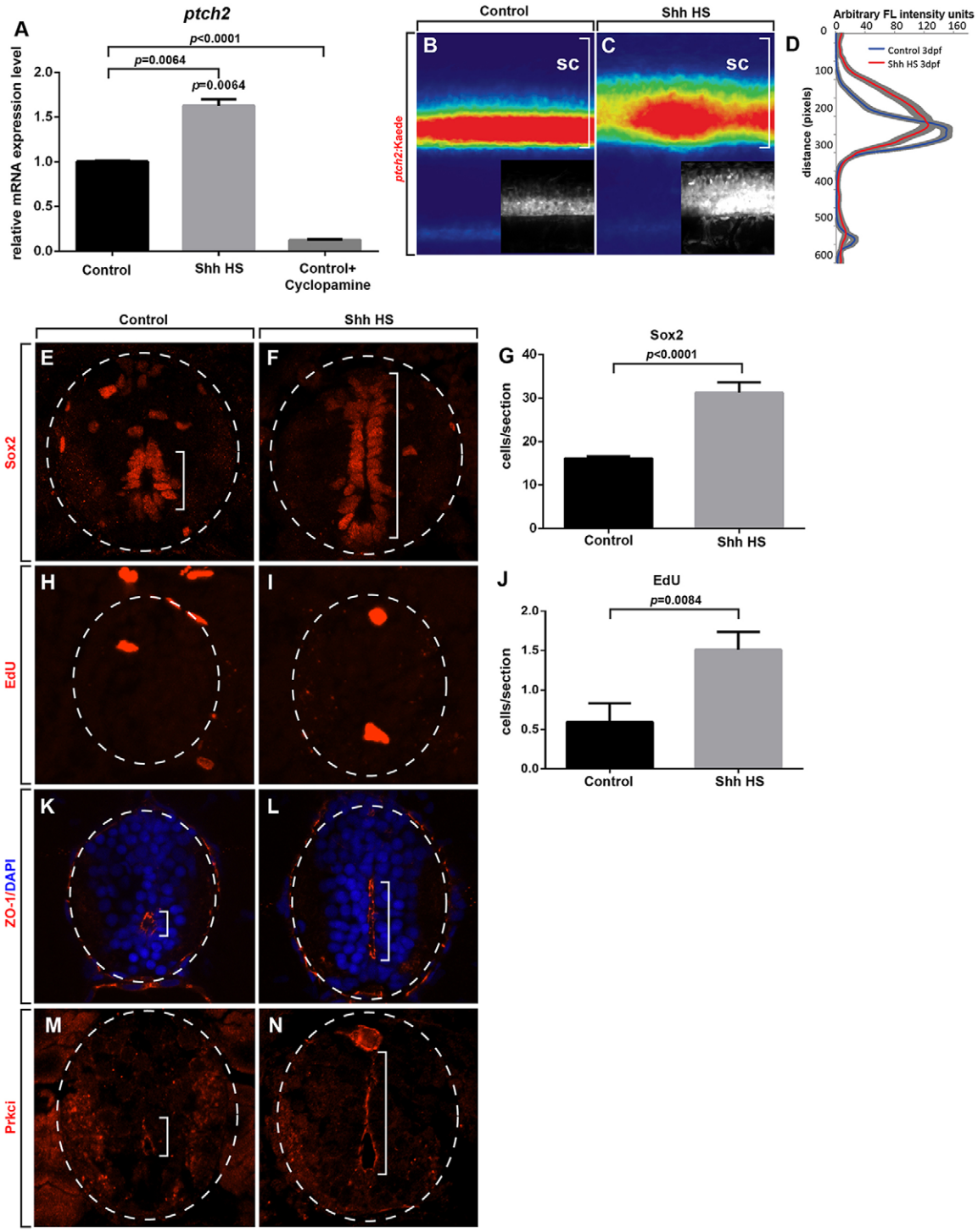

Fig. 3. Shh overexpression phenocopies loss of miR-219 function. (A) Graph showing that 3 dpf heatshocked *Tg(hsp70l:Shha-EGFP)* (Shh HS) larvae express *ptch2* at higher levels than controls and that cyclopamine treatment almost abolishes *ptch2* mRNA levels. Data represent the mean± s.e.m. (n=2 biological replicate experiments, consisting of 15-20 larvae, each). Significance calculated using an unpaired t-test. (B,C) Heat maps showing the average normalized fluorescence profile of control (n=21) and Shh HS (n=21) spinal cord (sc, brackets) *ptch2*:Kaede expression at 3 dpf, straightened and aligned along the dorsoventral axis. Dorsal is to the top. All heat maps display in the range of 0-150 arbitrary fluorescence units (blue to red). Insets show representative maximum projection images of confocal stacks obtained from single larvae. (D) Average normalized fluorescence profile of *ptch2*:Kaede generated by creating line scans along the dorsoventral axis. The solid colored lines (red and blue) represent the average normalized fluorescence profile at each pixel along the dorsoventral axis whereas the grey lines represent the s.e.m. at each pixel. Control (E,H,K,M) and heat-shocked *Tg(hsp701:Shha:EGFP)* (Shh HS) (F,I,L,N) embryos shown in transverse section with dorsal up. Dashed circles outline the spinal cord and brackets indicate the central canal/primitive lumen. (E,F) Immunohistochemistry to detect neural progenitors, marked by Sox2 expression. (G) Graph showing the number of $Sox2^+$ cells in control and Shh-overexpressing embryos. Data represent the mean±s.e.m. (n=15 embryos per group from 3 independent experiments). Significance calculated using an unpaired t-test. (H,I) EdU incorporation to detect dividing neural progenitors. (J) Graph showing the number of EdU^+ cells in the spinal cord at 3 dpf. Data represent the mean±s.e.m. (n=20 embryos per group). Significance calculated using an unpaired t-test. (K-N) 3 dpf Shh-overexpressing embryos maintain a primitive lumen marked by apically localized ZO-1 and Prkci.

Development (2016) 143, 2292-2304 doi:10.1242/dev.137844

Apical Par proteins regulate ciliogenesis

Our data support the hypothesis that reduction of apical Par proteins near the end of embryogenesis reduces the Hh signaling response, thereby triggering exit of neural progenitors from the cell cycle. What remains unclear, however, is how apical Par proteins regulate Hh signaling. Because previous data indicated that Par proteins could promote ciliogenesis and primary cilia are known signaling centers for Hh signaling, we predicted that apical Par proteins promote neural tube Shh signaling by regulating ciliogenesis. To test this, we evaluated primary cilia length using transgenic *Tg(βact::arl13b-GFP)* zebrafish, which express the ciliary protein Arl13b fused to GFP under the control of *actb1* (*β-actin*) regulatory DNA (Borovina et al., 2010). We injected *Tg(βact::arl13b-GFP)* embryos with miR-219 MO and found that primary cilia of the trunk spinal cord were significantly longer than cilia in control embryos (Fig. 5A,B,D). By contrast, cilia were significantly shorter in *prkci* mutant embryos than in control embryos (Fig. 5C,D). Are cilia longer in miR-219-deficient embryos because apical Par proteins are elevated? To test this possibility, we injected *prkci* mutant embryos with miR-219 MO. Cilia length in miR-219- and *prkci*-deficient embryos was similar to that of uninjected *prkci* mutant embryos (Fig. 5D), suggesting that miR-219 modulation of cilia length is mediated by apical Par protein function. To test whether or not miR-219 regulates cilia lengthening via its apical Par protein targets, we injected embryos with miR-219 target protector MOs and measured cilia length. Injections of both *prkci* TP MO and *pard* TP MO resulted in longer cilia (Fig. 5E), similar to loss of miR-219. These data indicate that miR-219 downregulation of apical Par polarity proteins reduces primary cilia length.

Because the rate or timing of cilia formation relative to cell division might influence Hh signaling, we performed live imaging to directly observe cilia growth over time. To do this, we created the constructs *sox19a:arl13b-GFP* and *sox19a:mCherry-CaaX*, which use *sox19a* regulatory DNA to express cilia and membrane markers in neural progenitors. We co-injected these constructs into newly fertilized zebrafish eggs and screened the embryos at 24 hpf for doubly labeled spinal cord cells, which we then followed using time-lapse confocal microscopy. As cells divided, cilia were retracted (Fig. 5G-I) and then quickly reformed (Fig. 5K). By measuring the rate of cilia regrowth following division, we found that cilia extended more rapidly in miR-219 MO-injected embryos than in control embryos (Fig. 5N). Most of the accelerated growth in miR-219 MO-injected embryos occurred in the first 30 min, raising the possibility that Par proteins promote initiation of ciliogenesis. Consistent with the static cilia length measurements above (Fig. 5A,D), the cilia were also longer in miR-219 MO-injected embryos at the end of the imaging period (Fig. 5N).

Our data provide evidence that downregulation of apical Par proteins by miR-219 reduces cilia length and growth rate, dampens the Hh signaling response and promotes the loss of neural progenitor characteristics. Does modulation of cilia dynamics account for modulation of Hh signaling and cell cycle exit? Mouse embryos lacking cilia are nearly devoid of Hh signaling (Huangfu et al., 2003; May et al., 2005) and mouse mutations that alter cilia formation also disrupt Hh signaling (Gray et al., 2009; Heydeck et al., 2009; Zeng et al., 2010) suggesting that regulation of ciliogenesis could have corresponding effects on Hh signaling. Zebrafish embryos that lack functions of Ift88 or Talpid3 have no primary cilia and are deficient for high-level Hh signaling but have expanded low-level signaling (Ben et al., 2011; Huang and Schier, 2009), suggesting that in zebrafish, cilia promote efficient Hh signaling. To test whether or not primary cilia, independent of apical Par protein functions, are necessary for neural progenitor maintenance, we examined *dzip1* mutant embryos, which lack primary cilia and have a Hh signaling profile similar to that of Ift88 and Talpid3-deficient embryos (Wolff et al., 2004; Sekimizu et al., 2004; Kim et al., 2010; Huang and Schier, 2009; Tay et al., 2010). At 3 and 5 dpf, *dzip1* mutant animals had similar numbers of $Sox2^+$ and $PH3^+$ spinal cord cells as the wild type (Fig. 6A-H), indicating that the lack of primary cilia does not cause depletion of neural progenitors. Thus, the low level of Hh signaling in *dzip1* mutant embryos is sufficient to maintain neural progenitors. These results raise the possibility that apical Par proteins maintain Hh signaling and neural progenitors via cilia-dependent and -independent mechanisms.

DISCUSSION

A key element of brain size and complexity is the regulated transition of dividing neural progenitors to differentiated neurons and glia. Neuroepithelial progenitors have apicobasal polarity, which can determine how progenitors respond to extracellular signals by subcellularly localizing signal reception and processing machinery. Here, we provide evidence that miR-219-mediated downregulation of apical Par polarity proteins helps trigger the transition from proliferation to differentiation by diminishing the progenitor cell response to Shh.

Because Shh reception and signal processing occur at apically positioned primary cilia of vertebrate epithelial cells, we reasoned that one way the proliferation to differentiation transition could be controlled is through regulation of apical membrane characteristics. Consistent with this, apical Par proteins localized to and promoted formation of cilia in cultured cells (Fan et al., 2004; Sfakianos et al., 2007) and reduction of Pard3 function reduced the length of photoreceptor cell cilia in zebrafish embryos (Krock and Perkins, 2014). In zebrafish embryos, Prkci and Pard3 localize to the apical membranes of dividing spinal cord progenitors but become depleted as the progenitors differentiate (Hudish et al., 2013; Ravanelli and Appel, 2015). These observations raise the possibility that modulation of the abundance and localization of apical Par protein can tune the Hh signaling response by modulating ciliogenesis or other apical membrane characteristics.

Following our previous work showing that miR-219 promotes differentiation of spinal cord progenitors by downregulating Pard3 and Prkci (Hudish et al., 2013), we began this study by investigating whether or not miR-219 function regulates Hh signaling. Indeed, loss of miR-219 function elevated the Hh signaling response, but only if Par protein functions were intact. Although miR-219 potentially targets many RNAs, the results of our *pard3* and *prkci* target protector MO experiments provide compelling evidence that miR-219-mediated Hh signaling is determined primarily by regulation of Pard3 and Prkci levels. miR-219-deficient embryos maintained excess spinal cord progenitors, but only if Hh signaling was intact, and forced expression of Shh phenocopied miR-219 loss of function. Our data also revealed that inhibition of Hh signaling depleted Prkci from apical membranes of dorsal spinal cord cells, raising the possibility that apical Par proteins and Hh signaling engage in a positive regulatory loop to maintain neural progenitors. Consistent with this possibility, recent data show that Gli1 promotes *prkci* transcription by directly binding DNA regulatory elements (Atwood et al., 2013). Altogether, our observations suggest that miR-219 breaks the positive feedback loop between apical Par proteins and Hh signaling to initiate neural progenitor cell cycle exit. In the chick neural tube, apical abscission separates apical Par proteins from progenitors prior to neuronal differentiation

Development (2016) 143, 2292-2304 doi:10.1242/dev.137844

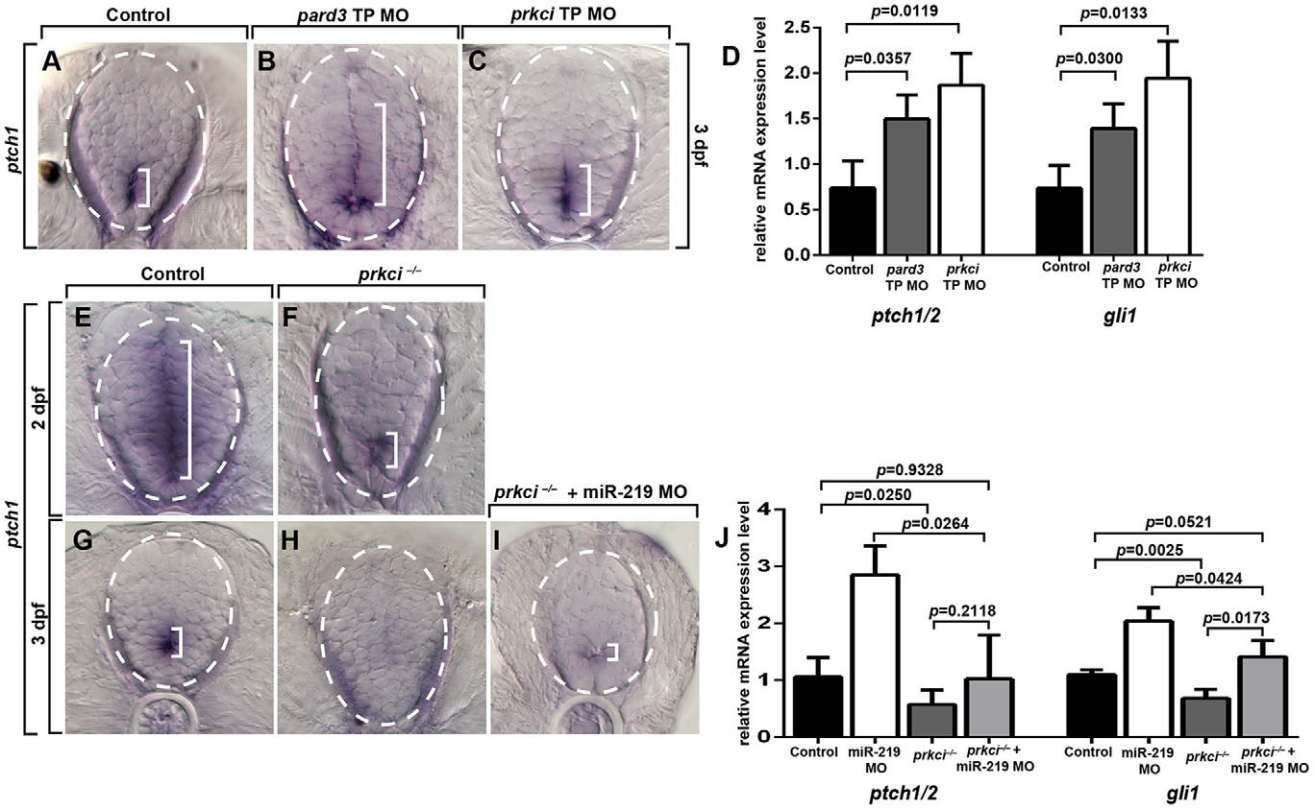

Fig. 4. Apical Par proteins mediate the effects of miR-219 function on Hh signaling. (A-C) *In situ* RNA hybridization to detect *ptch2* expression in 3 dpf control, *pard3* TP MO-injected and *prkci* TP MO-injected embryos. Dashed circles outline the spinal cord and brackets mark *ptch2* expression domain. (D) Graph showing relative *ptch2* and *gli1* RNA levels measured by qPCR. Data represent the mean±s.e.m. (n=3-5 biological replicates, consisting of 15-20 pooled embryos). Significance calculated using an unpaired t-test. (E-I) *In situ* RNA hybridization reveals reduced *ptch2* levels in 2 dpf and 3 dpf *prkci* mutant embryos and *prkci* mutant embryos injected with miR-219 MO. (J) Graph showing relative *ptch2* and *gli1* expression levels measured by qPCR. Data represent the mean±s.e.m. (n=3 biological replicates consisting of 15-20 pooled embryos, each). Significance calculated using an unpaired t-test.

(Das and Storey, 2014), suggesting that several distinct mechanisms operate to drive neuroepithelial progenitors into a differentiation pathway.

A potential mechanistic link between apical Par protein function and Hh signaling was uncovered by our time-lapse imaging studies of ciliogenesis. In particular, reducing miR-219 function and blocking access of miR-219 to its target sites on *pard3* and *prkci* mRNAs increased the length of spinal cord primary cilia and the rate at which spinal cord progenitors elongated cilia. Thus, longer and faster-forming primary cilia correlated with elevated Hh signaling, consistent with recent observations of cilia length and Hh signaling in cultured fibroblasts and mouse neural tube (Stasiulewicz et al., 2015). By contrast, *prkci* mutant embryos had shorter cilia, correlating with reduced Hh signaling. These observations suggested the intriguing possibility that cilia dynamics, regulated by apical Par proteins, tunes Hh signaling strength and thereby determines progenitor fate. However, we found that *dzip1* mutant embryos, which lack primary cilia (Glazer et al., 2010; Huang and Schier, 2009; Tay et al., 2010), had apparently normal numbers of spinal cord progenitors. Whereas Hh signaling is active in *dzip1* mutant embryos, albeit at reduced levels, our data indicate that Hh signaling is substantially reduced in *prkci* mutant embryos. Thus, the absence of apical Par protein functions might have a more dramatic effect on Hh signaling than the lack of primary cilia does, suggesting that Par protein-mediated modulation of Hh signaling occurs both by modulating cilia dynamics and via cilia-independent mechanisms.

How else might apical Par proteins promote Hh signaling? One possibility is that they do so by regulating Notch signaling, which can maintain neural progenitor fate. In support of this, depletion of Pard3 from developing mouse neocortex reduced Notch signaling and caused dividing cells to undergo neuronal differentiation (Bultje et al., 2009). Pard3 binds Numb (Nishimura and Kaibuchi, 2007), which negatively regulates Notch activity (Knoblich et al., 1995; Rhyu et al., 1994), and Numb and Numb-like are required for Pard3 regulation of Notch in the mouse neocortex (Bultje et al., 2009). Thus, Pard3 might promote Notch signaling and progenitor fate by preventing Numb and Numb-like from blocking Notch activity. Notably, recent data indicate that Notch signaling promotes Hh signaling in the neural tube by promoting localization of Ptch1 and Smo to cilia and cilia length (Kong et al., 2015; Stasiulewicz et al., 2015). Additionally, studies of basal cell carcinomas revealed that Prkci can phosphorylate and activate Gli1, thereby potentiating Hh signaling (Atwood et al., 2013). Similarly, in flies, aPKC, a Prkci homolog, can phosphorylate and activate Smo and the Gli homolog Ci, leading to expression of Hh target genes, including aPKC (Jiang et al., 2014b). Thus, the apical Par polarity protein complex might regulate Hh signaling directly, via Gli1 activation, and indirectly, via modulation of cilia dynamics. The role of cilia in mediating Hh signaling appears to differ in mice and zebrafish in that defective ciliogenesis significantly abrogates Hh signaling in mice (Huangfu et al., 2003; May et al., 2005) whereas it dampens but also expands Hh signaling in zebrafish (Ben et al., 2011; Huang and Schier, 2009). Perhaps the relative roles of direct and indirect modulation of

Development (2016) 143, 2292-2304 doi:10.1242/dev.137844

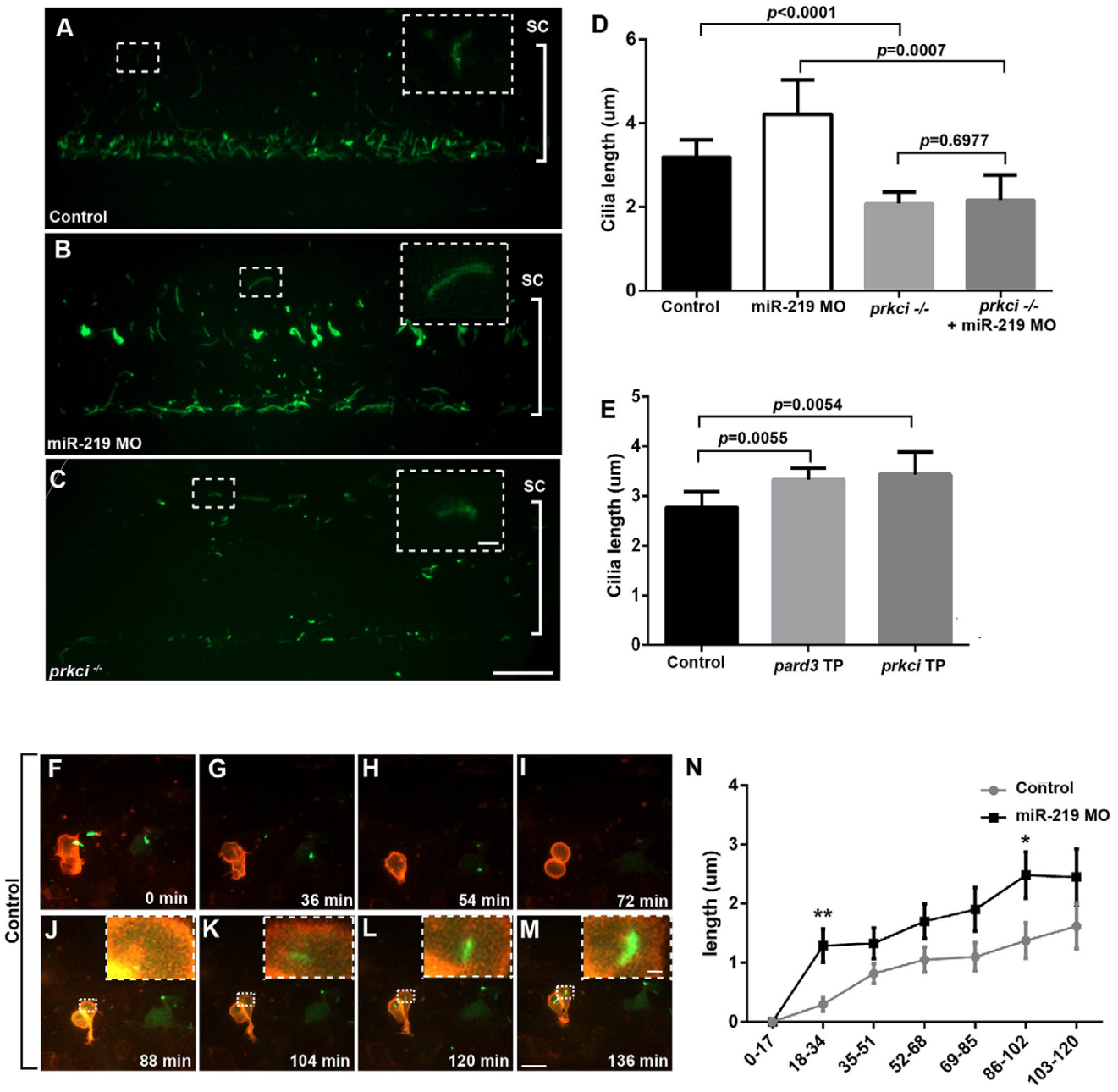

Fig. 5. Apical Par proteins regulate primary ciliogenesis. (A-C) Lateral images of living 3 dpf *Tg(βact::Arl13b–GFP)* embryos, focused on the trunk spinal cord. Scale bar: 20 µm. Brackets mark the spinal cord (sc) and outlined boxes show digital enlargements of primary cilia. The long motile cilia in ventral spinal cord were not used for these analyses. Scale bar: 1 µm. (D) Graph showing cilia length. Data represent the mean±s.e.m. (n=30 embryos from 3 independent experiments for each group and 10-30 cilia measured in each embryo). Significance calculated using an unpaired t-test. (E) Graph showing cilia length in 3 dpf control, *pard3* TP MO-injected and *prkci* TP MO-injected embryos. Data represent the mean±s.e.m. (n=30 embryos from 3 independent experiments for each group, and 10-30 cilia measured in each embryo). Significance calculated using an unpaired t-test. (F-M) Confocal images captured from time-lapse movies of dividing cells in the trunk spinal cord of a control embryo, beginning at 24 hpf. Time elapsed from the start of the movie is indicated on each panel. Cilia are labeled by Arl13b-EGFP and cell membranes are marked by membrane-tethered mCherry. Scale bar: 10 µm. Outlined boxes show digital enlargements of cilia. Scale bar: 1 µm. (N) Graph showing average cilia length (µm) over 120 min and outlined boxes show digital enlargements of cilia. The 0 min time point corresponds to the 88 min time point in J. Slope shows the rate of cilia growth is greater in miR-219 MO-injected embryos than in controls. Data represent the mean±s.e.m. (n=7 cells from 7 embryos for both conditions). Significance calculated using unpaired t-test. $^{**}P$=0.01959, $^{*}P$=0.0527.

Hh signaling by apical Par proteins differs in mice and zebrafish, accounting for distinct cilia defect-associated phenotypes.

Could miR-219 also regulate Hh signaling by targeting mRNAs that encode pathway components? Numerous studies have shown that various Hh pathway genes are targets of microRNAs in development and cancer (Akhtar et al., 2015; Flynt et al., 2007; Gao et al., 2013a,b; Jiang et al., 2014a; Ketley et al., 2013; Li et al., 2012; Wen et al., 2015; Wu et al., 2012; Yu et al., 2015; Zhang et al., 2015). Target prediction analysis identified a single potential miR-219 binding site within the 3′ UTR sequence of zebrafish *smoothened* (*smo*) mRNA, but not in other pathway members. Although we do not yet know whether *smo* is a functional target, this raises the possibility that miR-219 regulates the Hh signaling response by coordinately regulating transcripts encoding apical Par polarity proteins and Smo.

Development (2016) 143, 2292-2304 doi:10.1242/dev.137844

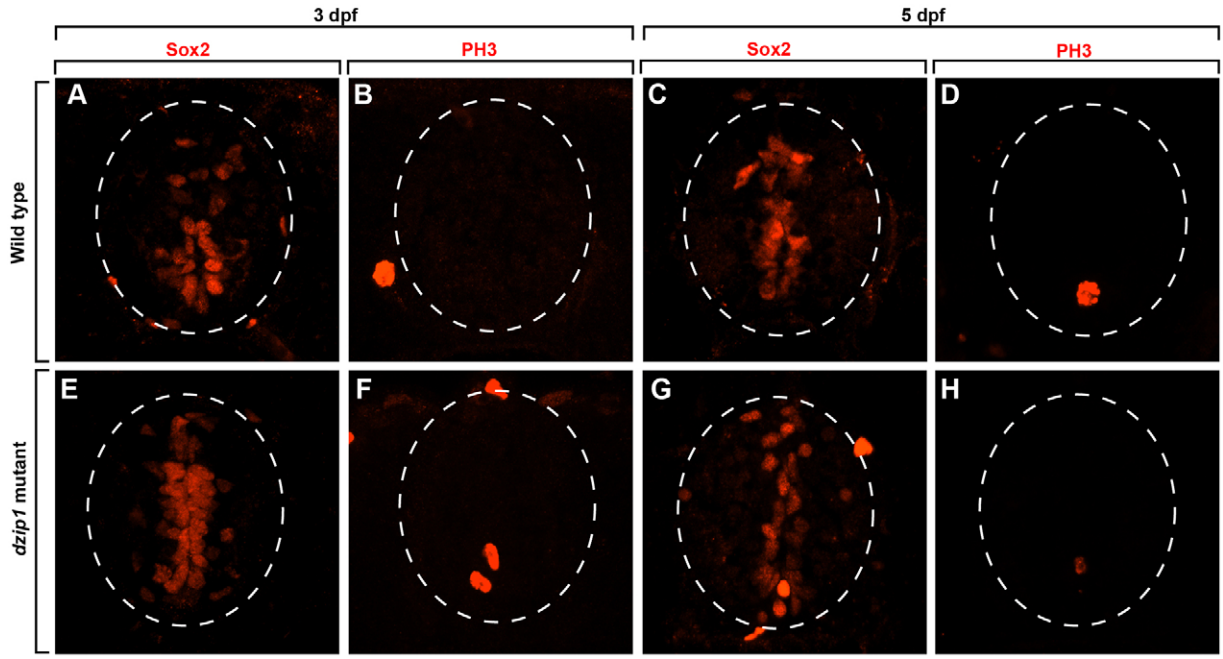

Fig. 6. Cilia-deficient mutant embryos have normal numbers of neural progenitors. (A-H) All images show representative transverse sections through trunk spinal cords of 3 and 5 dpf embryos with dorsal up. Dashed circles outline spinal cords. Representative images of control embryos at 3 dpf (A,B) and 5 dpf (C,D). Immunohistochemistry to detect neural progenitors marked by Sox2 expression (A,C) and phosphohistone H3 (PH3) to detect cells undergoing mitosis (B,D). *dzip* mutant embryos were also labeled with Sox2 at 3 dpf (E) and 5 dpf (G) and PH3 at 3 dpf (F) and 5 dpf (H).

Altogether, our data suggest that apical Par polarity proteins and Hh signaling engage in positive feedback regulation to maintain neural progenitors in a dividing, undifferentiated state. Initiation of miR-219 expression during the late stages of spinal cord development (Hudish et al., 2013) appears to break the feedback loop cycle by depleting apical Par proteins, which dampens Par protein-dependent Hh signaling activity. Some childhood medulloblastomas express miR-219 at abnormally low levels relative to levels in neural stem cells (Ferretti et al., 2009; Genovesi et al., 2011), raising the possibility that failure to break a Par protein-Hh signaling feedback loop can contribute to tumor formation.

MATERIALS AND METHODS

Zebrafish husbandry

The University of Colorado Anschutz Medical Campus Institutional Animal Care and Use Committee approved all zebrafish studies. Embryos were produced by pair-wise mating and kept at 28.5°C in egg water or embryo medium (15 mM NaCl, 0.5 mM KCl, 1 mM $CaCl_2$, 1 mM $MgSO_4$, 0.15 mM KH_2PO_4, 0.05 mM NH_2PO_4, 0.7 mM $NaHCO_3$). Embryos were staged to hpf or days post-fertilization (dpf) according to established zebrafish guidelines (Kimmel et al., 1995). The experiments conducted in this study used the following strains of zebrafish: AB, *Tg(hsp701:Shha:EGFP)* (Shen et al., 2013) and *Tg(βact::Arl13b-GFP)* (Borovina et al., 2010), $dzip^{+/-}$ ($iguana^{ts294e}$) (Sekimizu et al., 2004), $prkci^{+/-}$ (has^{m567}) (Horne-Badovinac et al., 2001) and *Tg(ptch2:Kaede)* (Huang et al., 2012). Animals of either sex were used.

Immunohistochemistry

Embryos and larvae were fixed in 4% paraformaldehyde (PFA) overnight at 4°C. Fixed embryos were embedded in 1.5% agar with 5% sucrose and transferred to a 30% sucrose solution in scintillation vials and incubated at 4°C overnight. The blocks were then frozen and cut into 10-15 µm sections using a cryostat microtome. The sections were incubated with the following primary antibodies: rabbit anti-phosphohistone H3 (1:1000, 06-570, Millipore), rabbit anti-PkC (1:200, sc-216, Santa Cruz Biotechnology), mouse anti–ZO-1 (1:200, 33-9100, Invitrogen), rabbit anti-Sox2 (1:500, ab97959, Abcam). For fluorescent detection of antibody labeling, we used Alexa Fluor 568 and Alexa Fluor 647 goat anti-mouse and goat anti-rabbit secondary antibodies (1:200, Invitrogen). To detect EdU incorporation, we incubated the slides in 250 µl EdU Detection Reaction mix (Invitrogen) for 40 min at room temperature. Images were collected on a Zeiss Axio Observer microscope equipped with a PerkinElmer UltraVIEW VoX spinning disk confocal system and Volocity imaging software (PerkinElmer). Images were contrast enhanced using either Volocity or Photoshop (Adobe CS4).

In situ RNA hybridization

Embryos and larvae were fixed in 4% PFA overnight at 4°C and stored in methanol at −20°C. After linearizing plasmids with the appropriate restriction enzymes, antisense cRNA was transcribed using Roche digoxigenin-labeling reagents and T3, T7 or SP6 RNA polymerases (New England Biolabs). After processing embryos for *in situ* RNA hybridization, they were embedded in agar and sectioned as described above. Sections were rehydrated in 1× PBS for 30 min then covered with 75% glycerol. Images were obtained on a Zeiss Axio Observer microscope equipped with DIC optics, a Retiga Exi color camera and Volocity imaging software. Some images were contrast enhanced using Photoshop (Adobe CS4).

Morpholino oligonucleotide injections

Antisense morpholino oligonucleotides were purchased from Gene Tools, LLC. These included: miR-219 MO (5′-CAAGAATTGCGTTTG-GACAATCA-3′) (Zhao et al., 2010), *pard3* TP MO (5′-CTGATTGTCA-GAGCATCTCTACTAC-3′), control *pard3* TP MO (5′-ACAGAGTCAA-AGTGACGGACTCC-3′) and *prkci* TP MO (AAGCGACCGTCACACA-CTCCTCCGC) (Hudish et al., 2013). Morpholino oligonucleotides were dissolved in water to create stock solutions of 1 mM and diluted in 2× injection buffer (5 mg ml^{-1} Phenol Red, 40 mM HEPES and 240 mM KCl) to create a working injection concentration of 0.25 mM. All morpholinos were co-injected with 0.09 mM dose of *p53* MO. We injected 1-2 nl into the yolk just below the single cell of fertilized embryos. All morpholino oligonucleotide injected embryos were raised in embryo medium at 28.5°C. We previously validated the miR-219 MO using *pard3* and *prkci* 3′ UTR reporter assays and by showing that miR-219 MO phenotypes are dependent on Pard3 and Prkci functions (Hudish et al., 2013).

Development (2016) 143, 2292-2304 doi:10.1242/dev.137844

Plasmid construction and injections

Neural progenitors were labeled using a conserved regulatory DNA element near zebrafish *sox19a*, which is expressed by neural cells (Okuda et al., 2006). The 1554 bp *sox19a* 3′ regulatory element was amplified using the primers *AscI fwd* 5′-ggcgcgccTGTAAGCACACGGCCATTTA-3′ and *FseI rev* 5′-aaaggccggccTCACCTAACCCCGAGAAGAA-3′ and cloned into the Tol2 Gateway entry vector p5E-FAbasal using *Asc*I/*Fse*I (NEB) restriction enzyme sites as described previously (Kwan et al., 2007). Four-part Gateway cloning was used to construct the final vector *pEXPR-Tol2-sox19a:mCherry-CaaXpA-pA2* using LR Clonase II Plus Enzyme Mix (Invitrogen 12538-120) and *pME-mCherry-CaaX, p3E-polyA*, and *pDEST-Tol2-pA2* vectors as described previously (Kwan et al., 2007). The *pME-Arl13b-EGFP* vector was created by subcloning *Arl13b-EGFP* from a *pCS2-Arl13b-EGFP* plasmid (gift from Brian Ciruna, The Hospital for Sick Children, Toronto, Ontario, Canada) by traditional cloning using the *Pst*I and *Bam*HI restriction sites. Multisite Gateway cloning was used to create *pEXPR-Tol2-sox19a:Arl13b-EGFP-pA2* as described above. Embryos were injected at the single-cell stage with 1 nl of 50 ng/µl plasmid DNA in 0.2 M KCl and sorted for GFP^+/mCherry-$CaaX^+$ neural progenitors at 24 hpf.

EdU labeling

Dechorionated embryos were labeled with 5-ethynyl-2′-deoxyuridine (EdU). Embryos were incubated in 2 mM EdU (Click-iT EdU AlexaFluor 555 detection kit; Invitrogen, c10338) in embryo medium with 10% DMSO for 30 min at room temperature. The fish were then fixed in 4% PFA in PBS with 116 mM sucrose and 150 µM $CaCl_2$ at 4°C overnight.

Heat shock procedure

Tg(hsp701:Shha:EGFP) and non-transgenic control embryos were placed in a 50 ml beaker in approximately 10 ml of embryo medium and immersed in a 38°C water bath for 30 min after which they were allowed to recover at RT for 20 min and were placed back in the incubator afterwards. Heat shock was performed at 24, 32, 48 and 56 hpf to keep transgene expression high. Embryos were fixed at 72 hpf and processed for immunohistochemistry as described above.

Tg(ptch2:Kaede) conversion and image analysis

Tg(hsp701:Shha:EGFP);Tg(ptch2:Kaede) embryos were heat shocked as described above. At 3 dpf, embryos were mounted in low-melting temperature agarose and illuminated with UV from a mercury bulb source for 1 min per embryo. Immediately afterward, photoconversion was confirmed by assessing both red and green fluorescence. *z*-stack images were obtained of the trunk spinal cord above the yolk extension using a 20× objective mounted on the confocal microscope described above. The fluorescence distribution of the *ptch2*:Kaede reporter was analyzed using ImageJ/Fiji. Briefly, maximum intensity projections for each spinal cord were manually straightened and aligned along the bottom edge of the major strip of Kaede fluorescence intensity in the ventral spinal cord. Next, each image was background subtracted and normalized to the maximum signal within the major strip of Kaede intensity to generate 8-bit images displaying the same intensity range. Finally, a 500 pixel wide (149 µm) line-scan was generated along the dorsoventral axis of each image. For each pixel position along the linescan, the average pixel intensity and the standard error of the mean were plotted for all averaged spinal cords within an experimental condition. The average stack projector plug-in was used to generate the average images, which were displayed using the 'physics' look-up table. All images are displayed within the range of 0-150 arbitrary intensity units.

Quantitative PCR

RNA was isolated from 15-20 pooled larvae for each control or experimental condition. Samples for each condition were collected in triplicate. Reverse transcription was performed using the iScript Reverse Transcriptase Supermix for RT-PCR (Bio-Rad, 1708840). Real-time qPCR was performed in triplicate for each cDNA sample using an Applied Biosystems StepOne Plus machine and software v.2.1. TaqMan Assays were used to detect *patched2* (Dr03118687_m1), *gli1* (Dr03093669_m1) and endogenous control *rpl13a* (Dr03101115_g1).

Quantification and statistical analysis

No animals were excluded from analysis. For some experiments, only a subset of animals was used for quantification, but these were chosen at random. Animals were randomly assigned to control and experimental groups. Cell counts were obtained by direct observation of sections using the microscopes described above. For Sox2, EdU and PH-3, 10 sections per embryo from 15 embryos per group with two or three replicates were counted to produce the average number per section. *P* values were generated using an unpaired *t*-test using GraphPad Prism software.

Quantification of static primary cilia length and rate of formation *in vivo*

All measurements were made using spinal cord primary cilia and not the longer motile cilia of the floor plate. Time-lapse imaging was performed on control and miR-219-injected embryos with frames captured at least every 17 min, for a total of 120 min. For both static and live cilia length measurements, primary cilia length was measured on maximum intensity projections in Volocity or in ImageJ using a custom script to automate use of the polyline tool. For live measurements, length was measured at every point after a cell divided, except for cases where the cilium reoriented along the *z*-axis, which is difficult to measure accurately. The cilia length was binned into 17 min intervals and averaged. The rate of cilia formation was calculated between each binned time interval and significance was assessed with an unpaired *t*-test.

Cyclopamine treatments

Cyclopamine was reconstituted in 100% ethanol at a stock concentration of 10 mM and diluted fresh for every treatment. Approximately 20-25 embryos were placed in glass dishes and treated with 50 µM cyclopamine (Cayman Chemicals) or 0.5% ethanol starting at 24 hpf. Embryos were placed in the incubator in the cyclopamine or control solutions until 3 dpf at which point they were fixed and analyzed.

Acknowledgements

We thank members of the Appel laboratory for valuable discussions and Christina Kearns for technical assistance. We are grateful for the gifts of the transgenic line *Tg(hsp701:Shha:EGFP)* from Rolf Karlstrom, the *Tg(βact::Arl13b-GFP)* transgenic line from Thomas Schilling and the *Arl13b-GFP* plasmid from Brian Ciruna.

Competing interests

The authors declare no competing or financial interests.

Author contributions

L.I.H. performed all the experiments and analyzed the data. D.F.G. and C.G.P. provided important advice, macros and instruction for analysis and quantification of cilia growth and *ptch2*:Kaede fluorescence intensity analyses. A.M.R. cloned and characterized *sox19a* regulatory DNA. P.H. provided *dzip1* mutant embryos and important advice. L.I.H. and B.A. conceived the project and wrote the manuscript.

Funding

This work was supported by the National Institutes of Health (NIH) [R01 NS046668] and a gift from the Gates Frontiers Fund to B.A. A.M.R was supported by an NIH National Cancer Research Institute fellowship [T32 5T32CA08208613]. C.G.P. was supported by the NIH National Institute of General Medical Sciences [GM0099820], the Boettcher Webb-Waring Foundation and the Pew Biomedical Scholars Program. P.H. was supported by a Natural Sciences and Engineering Research Council of Canada (NSERC) Discovery Grant. The University of Colorado Anschutz Medical Campus Zebrafish Core Facility was supported by the NIH [P30 NS048154]. Deposited in PMC for deposition after 12 months.

References

Afonso, C. and Henrique, D. (2006). PAR3 acts as a molecular organizer to define the apical domain of chick neuroepithelial cells. *J. Cell Sci.* **119**, 4293-4304.

Akhtar, N., Makki, M. S. and Haqqi, T. M. (2015). MicroRNA-602 and microRNA-608 regulate sonic hedgehog expression via target sites in the coding region in human chondrocytes. *Arthritis Rheum.* **67**, 423-434.

Atwood, S. X., Li, M., Lee, A., Tang, J. Y. and Oro, A. E. (2013). GLI activation by atypical protein kinase C ι/λ regulates the growth of basal cell carcinomas. *Nature* **494**, 484-488.

Aza-Blanc, P., Ramírez-Weber, F.-A., Laget, M.-P., Schwartz, C. and Kornberg, T. B. (1997). Proteolysis that is inhibited by hedgehog targets Cubitus interruptus protein to the nucleus and converts it to a repressor. *Cell* **89**, 1043-1053.

Ben, J., Elworthy, S., Ng, A. S. M., van Eeden, F. and Ingham, P. W. (2011). Targeted mutation of the talpid3 gene in zebrafish reveals its conserved requirement for ciliogenesis and Hedgehog signalling across the vertebrates. *Development* **138**, 4969-4978.
Borovina, A., Superina, S., Voskas, D. and Ciruna, B. (2010). Vangl2 directs the posterior tilting and asymmetric localization of motile primary cilia. *Nat. Cell Biol.* **12**, 407-412.
Bultje, R. S., Castaneda-Castellanos, D. R., Jan, L. Y., Jan, Y.-N., Kriegstein, A. R. and Shi, S.-H. (2009). Mammalian Par3 regulates progenitor cell asymmetric division via notch signaling in the developing neocortex. *Neuron* **63**, 189-202.
Chen, J. and Zhang, M. (2013). The Par3/Par6/aPKC complex and epithelial cell polarity. *Exp. Cell Res.* **319**, 1357-1364.
Chen, J. K., Taipale, J., Cooper, M. K. and Beachy, P. A. (2002). Inhibition of Hedgehog signaling by direct binding of cyclopamine to Smoothened. *Genes Dev.* **16**, 2743-2748.
Concordet, J., Lewis, K. E., Moore, J. W., Goodrich, L. V., Johnson, R. L., Scott, M. P. and Ingham, P. W. (1996). Spatial regulation of a zebrafish patched homologue reflects the roles of sonic hedgehog and protein kinase A in neural tube and somite patterning. *Development* **2846**, 2835-2846.
Costa, M. R., Wen, G., Lepier, A., Schroeder, T. and Götz, M. (2008). Par-complex proteins promote proliferative progenitor divisions in the developing mouse cerebral cortex. *Development* **135**, 11-22.
Dahmane, N. and Ruiz, A. (1999). Sonic hedgehog and cerebellum development. *Development* **3100**, 3089-3100.
Das, R. M. and Storey, K. G. (2014). Apical Abscission Alters Cell Polarity and Dismantles the Primary Cilium During Neurogenesis. *Science* **343**, 200-204.
Dessaud, E., McMahon, A. P. and Briscoe, J. (2008). Pattern formation in the vertebrate neural tube: a sonic hedgehog morphogen-regulated transcriptional network. *Development* **135**, 2489-2503.
Ellis, P., Fagan, B. M., Magness, S. T., Hutton, S., Taranova, O., Hayashi, S., McMahon, A., Rao, M. and Pevny, L. (2004). SOX2, a persistent marker for multipotential neural stem cells derived from embryonic stem cells, the embryo or the adult. *Dev. Neurosci.* **26**, 148-165.
Fan, S., Hurd, T. W., Liu, C.-J., Straight, S. W., Weimbs, T., Hurd, E. A., Domino, S. E., Margolis, B. and Arbor, A. (2004). Polarity proteins control ciliogenesis via kinesin motor interactions. *Curr. Biol.* **14**, 1451-1461.
Ferretti, E., De Smaele, E., Po, A., Di Marcotullio, L., Tosi, E., Espinola, M. S. B., Di Rocco, C., Riccardi, R., Giangaspero, F., Farcomeni, A. et al. (2009). MicroRNA profiling in human medulloblastoma. *Int. J. Cancer* **124**, 568-577.
Flynt, A. S., Li, N., Thatcher, E. J., Solnica-Krezel, L. and Patton, J. G. (2007). Zebrafish miR-214 modulates Hedgehog signaling to specify muscle cell fate. *Nat. Genet.* **39**, 259-263.
Gao, L., Hou, X., Wu, L., Zhang, F., Zhang, Q., Ye, X., Yang, Y. and Lin, X. (2013a). Drosophila miR-960 negatively regulates Hedgehog signaling by suppressing Smoothened, Costal-2 and Fused. *Cell. Signal.* **25**, 1301-1309.
Gao, L., Wu, L., Hou, X., Zhang, Q., Zhang, F., Ye, X., Yang, Y. and Lin, X. (2013b). Drosophila miR-932 modulates hedgehog signaling by targeting its co-receptor Brother of ihog. *Dev. Biol.* **377**, 166-176.
Genovesi, L. A., Carter, K. W., Gottardo, N. G., Giles, K. M. and Dallas, P. B. (2011). Integrated analysis of miRNA and mRNA expression in childhood medulloblastoma compared with neural stem cells. *PLoS ONE* **6**, e23935.
Glazer, A. M., Wilkinson, A. W., Backer, C. B., Lapan, S. W., Gutzman, J. H., Cheeseman, I. M. and Reddien, P. W. (2010). The Zn Finger protein Iguana impacts Hedgehog signaling by promoting ciliogenesis. *Dev. Biol.* **337**, 148-156.
Gray, R. S., Abitua, P. B., Wlodarczyk, B. J., Szabo-Rogers, H. L., Blanchard, O., Lee, I., Weiss, G. S., Liu, K. J., Marcotte, E. M., Wallingford, J. B. et al. (2009). The planar cell polarity effector Fuz is essential for targeted membrane trafficking, ciliogenesis and mouse embryonic development. *Nat. Cell Biol.* **11**, 1225-1232.
Heydeck, W., Zeng, H. and Liu, A. (2009). Planar cell polarity effector gene Fuzzy regulates cilia formation and Hedgehog signal transduction in mouse. *Dev. Dyn.* **238**, 3035-3042.
Horne-Badovinac, S., Lin, D., Waldron, S., Schwarz, M., Mbamalu, G., Pawson, T., Jan, Y.-N., Stainier, D. Y. R. and Abdelilah-Seyfried, S. (2001). Positional cloning of heart and soul reveals multiple roles for PKC lambda in zebrafish organogenesis. *Curr. Biol.* **11**, 1492-1502.
Huang, P. and Schier, A. F. (2009). Dampened Hedgehog signaling but normal Wnt signaling in zebrafish without cilia. *Development* **136**, 3089-3098.
Huang, P., Xiong, F., Megason, S. G. and Schier, A. F. (2012). Attenuation of Notch and Hedgehog signaling is required for fate specification in the spinal cord. *PLoS Genet.* **8**, e1002762.
Huangfu, D., Liu, A., Rakeman, A. S., Murcia, N. S., Niswander, L. and Anderson, K. V. (2003). Hedgehog signalling in the mouse requires intraflagellar transport proteins. *Nature* **426**, 83-87.
Hudish, L. I., Blasky, A. J. and Appel, B. (2013). miR-219 regulates neural precursor differentiation by direct inhibition of apical par polarity proteins. *Dev. Cell* **27**, 387-398.
Ishikawa, H. and Marshall, W. F. (2011). Ciliogenesis: building the cell's antenna. *Nat. Rev. Mol. Cell Biol.* **12**, 222-234.
Jensen, A. M. and Wallace, V. A. (1997). Expression of Sonic hedgehog and its putative role as a precursor cell mitogen in the developing mouse retina. *Development* **124**, 363-371.
Jeong, J. and McMahon, A. P. (2005). Growth and pattern of the mammalian neural tube are governed by partially overlapping feedback activities of the hedgehog antagonists patched 1 and Hhip1. *Development* **132**, 143-154.
Jessell, T. M. (2000). Neuronal specification in the spinal cord: inductive signals and transcriptional codes. *Nat. Rev. Genet.* **1**, 20-29.
Jiang, Z., Cushing, L., Ai, X. and Lü, J. (2014a). miR-326 is downstream of Sonic hedgehog signaling and regulates the expression of Gli2 and smoothened. *Am. J. Respir. Cell Mol. Biol.* **51**, 273-283.
Jiang, K., Liu, Y., Fan, J., Epperly, G., Gao, T., Jiang, J. and Jia, J. (2014b). Hedgehog-regulated atypical PKC promotes phosphorylation and activation of Smoothened and Cubitus interruptus in Drosophila. *Proc. Natl. Acad. Sci. USA* **111**, E4842-E4850.
Kenney, A. M. and Rowitch, D. H. (2000). Sonic hedgehog promotes G(1) cyclin expression and sustained cell cycle progression in mammalian neuronal precursors. *Mol. Cell. Biol.* **20**, 9055-9067.
Ketley, A., Warren, A., Holmes, E., Gering, M., Aboobaker, A. A. and Brook, J. D. (2013). The miR-30 microRNA family targets smoothened to regulate hedgehog signalling in zebrafish early muscle development. *PLoS ONE* **8**, e65170.
Kim, H. R., Richardson, J., van Eeden, F. and Ingham, P. W. (2010). Gli2a protein localization reveals a role for Iguana/DZIP1 in primary ciliogenesis and a dependence of Hedgehog signal transduction on primary cilia in the zebrafish. *BMC Biol.* **8**, 65.
Kimmel, C. B., Ballard, W. W., Kimmel, S. R., Ullmann, B. and Schilling, T. F. (1995). Stages of embryonic development of the zebrafish. *Dev. Dyn.* **203**, 253-310.
Knoblich, J. A., Jan, L. Y. and Jan, Y. N. (1995). Asymmetric segregation of Numb and Prospero during cell division. *Nature* **377**, 624-627.
Kong, J. H., Yang, L., Dessaud, E., Chuang, K., Moore, D. M., Rohatgi, R., Briscoe, J. and Novitch, B. G. (2015). Notch activity modulates the responsiveness of neural progenitors to sonic hedgehog signaling. *Dev. Cell* **33**, 373-387.
Kosodo, Y., Röper, K., Haubensak, W., Marzesco, A.-M., Corbeil, D. and Huttner, W. B. (2004). Asymmetric distribution of the apical plasma membrane during neurogenic divisions of mammalian neuroepithelial cells. *EMBO J.* **23**, 2314-2324.
Krock, B. L. and Perkins, B. D. (2014). The Par-PrkC polarity complex is required for cilia growth in zebrafish photoreceptors. *PLoS ONE* **9**, e104661.
Kwan, K. M., Fujimoto, E., Grabher, C., Mangum, B. D., Hardy, M. E., Campbell, D. S., Parant, J. M., Yost, H. J., Kanki, J. P. and Chien, C.-B. (2007). The Tol2kit: a multisite gateway-based construction kit for Tol2 transposon transgenesis constructs. *Dev. Dyn.* **236**, 3088-3099.
Le Dréau, G. and Martí, E. (2012). Dorsal-ventral patterning of the neural tube: a tale of three signals. *Dev. Neurobiol.* **72**, 1471-1481.
Lee, C.-Y., Robinson, K. J. and Doe, C. Q. (2006). Lgl, Pins and aPKC regulate neuroblast self-renewal versus differentiation. *Nature* **439**, 594-598.
Li, Y., Zhang, D., Chen, C., Ruan, Z., Li, Y. and Huang, Y. (2012). MicroRNA-212 displays tumor-promoting properties in non-small cell lung cancer cells and targets the hedgehog pathway receptor PTCH1. *Mol. Biol. Cell* **23**, 1423-1434.
Litingtung, Y. and Chiang, C. (2000). Specification of ventral neuron types is mediated by an antagonistic interaction between Shh and Gli3. *Nat. Neurosci.* **3**, 979-985.
May, S. R., Ashique, A. M., Karlen, M., Wang, B., Shen, Y., Zarbalis, K., Reiter, J., Ericson, J. and Peterson, A. S. (2005). Loss of the retrograde motor for IFT disrupts localization of Smo to cilia and prevents the expression of both activator and repressor functions of Gli. *Dev. Biol.* **287**, 378-389.
Nishimura, T. and Kaibuchi, K. (2007). Numb controls integrin endocytosis for directional cell migration with aPKC and PAR-3. *Dev. Cell* **13**, 15-28.
Okuda, Y., Yoda, H., Uchikawa, M., Furutani-Seiki, M., Takeda, H., Kondoh, H. and Kamachi, Y. (2006). Comparative genomic and expression analysis of group B1 sox genes in zebrafish indicates their diversification during vertebrate evolution. *Dev. Dyn.* **235**, 811-825.
Prehoda, K. E. (2009). Polarization of Drosophila neuroblasts during asymmetric division. *Cold Spring Harb. Perspect. Biol.* **1**, a001388.
Ravanelli, A. M. and Appel, B. (2015). Motor neurons and oligodendrocytes arise from distinct cell lineages by progenitor recruitment. *Genes Dev.* **29**, 2504-2515.
Rhyu, M. S., Jan, L. Y. and Jan, Y. N. (1994). Asymmetric distribution of numb protein during division of the sensory organ precursor cell confers distinct fates to daughter cells. *Cell* **76**, 477-491.
Rowitch, D. H., S-Jacques, B., Lee, S. M., Flax, J. D., Snyder, E. Y. and McMahon, A. P. (1999). Sonic hedgehog regulates proliferation and inhibits differentiation of CNS precursor cells. *J. Neurosci.* **19**, 8954-8965.
Sekimizu, K., Nishioka, N., Sasaki, H., Takeda, H., Karlstrom, R. O. and Kawakami, A. (2004). The zebrafish iguana locus encodes Dzip1, a novel zinc-finger protein required for proper regulation of Hedgehog signaling. *Development* **131**, 2521-2532.

Development (2016) 143, 2292-2304 doi:10.1242/dev.137844

Sfakianos, J., Togawa, A., Maday, S., Hull, M., Pypaert, M., Cantley, L., Toomre, D. and Mellman, I. (2007). Par3 functions in the biogenesis of the primary cilium in polarized epithelial cells. *J. Cell Biol.* **179**, 1133-1140.

Shen, M.-C., Ozacar, A. T., Osgood, M., Boeras, C., Pink, J., Thomas, J., Kohtz, J. D. and Karlstrom, R. (2013). Heat-shock-mediated conditional regulation of hedgehog/gli signaling in zebrafish. *Dev. Dyn.* **242**, 539-549.

Stasiulewicz, M., Gray, S., Mastromina, I., Silva, J. C., Björklund, M., Seymour, P. A., Booth, D., Thompson, C., Green, R., Hall, E. A. et al. (2015). A conserved role for Notch signaling in priming the cellular response to Shh through ciliary localisation of the key Shh transducer Smo. *Development* **142**, 2291-2303.

Tay, S. Y., Yu, X., Wong, K. N., Panse, P., Ng, C. P. and Roy, S. (2010). The iguana/DZIP1 protein is a novel component of the ciliogenic pathway essential for axonemal biogenesis. *Dev. Dyn.* **239**, 527-534.

Ulloa, F. and Briscoe, J. (2007). Morphogens and the control of cell proliferation and patterning in the spinal cord. *Cell Cycle* **6**, 2640-2649.

Wang, B., Fallon, J. F. and Beachy, P. A. (2000). Hedgehog-regulated processing of Gli3 produces an anterior/posterior repressor gradient in the developing vertebrate limb. *Cell* **100**, 423-434.

Wechsler-Reya, R. J. and Scott, M. P. (1999). Control of neuronal precursor proliferation in the cerebellum by sonic Hedgehog. *Neuron* **22**, 103-114.

Wen, S.-Y., Lin, Y., Yu, Y.-Q., Cao, S.-J., Zhang, R., Yang, X.-M., Li, J., Zhang, Y.-L., Wang, Y.-H., Ma, M.-Z. et al. (2015). miR-506 acts as a tumor suppressor by directly targeting the hedgehog pathway transcription factor Gli3 in human cervical cancer. *Oncogene* **34**, 717-725.

Wolff, C., Roy, S., Lewis, K. E., Schauerte, H., Joerg-Rauch, G., Kirn, A., Weiler, C., Geisler, R., Haffter, P. and Ingham, P. W. (2004). iguana encodes a novel zinc-finger protein with coiled-coil domains essential for Hedgehog signal transduction in the zebrafish embryo. *Genes Dev.* **18**, 1565-1576.

Wu, L.-F., Gao, L., Hou, X.-M., Zhang, Q.-H., Li, S., Yang, Y.-F. and Lin, X.-H. (2012). Drosophila miR-5 suppresses Hedgehog signaling by directly targeting Smoothened. *FEBS Lett.* **586**, 4052-4060.

Yu, F., Zheng, Y., Hong, W., Chen, B., Dong, P. and Zheng, J. (2015). MicroRNA–200a suppresses epithelial–to–mesenchymal transition in rat hepatic stellate cells via GLI family zinc finger 2. *Mol. Med. Rep.* **12**, 8121-8128.

Zeng, H., Hoover, A. N. and Liu, A. (2010). PCP effector gene Inturned is an important regulator of cilia formation and embryonic development in mammals. *Dev. Biol.* **339**, 418-428.

Zhang, X.-L., Shi, H.-J., Wang, J.-P., Tang, H.-S. and Cui, S.-Z. (2015). MiR-218 inhibits multidrug resistance (MDR) of gastric cancer cells by targeting Hedgehog/smoothened. *Int. J. Clin. Exp. Pathol.* **8**, 6397-6406.

Zhao, X., He, X., Han, X., Yu, Y., Ye, F., Chen, Y., Hoang, T., Xu, X., Mi, Q.-S., Xin, M. et al. (2010). MicroRNA-mediated control of oligodendrocyte differentiation. *Neuron* **65**, 612-626.